Effect of High Temperature on the Aqueous H_2S Corrosion of Mild Steel

Shujun Gao,[‡,] Peng Jin,[*] Bruce Brown,[*] David Young,[*] Srdjan Nešić,[*] and Marc Singer[*]*

ABSTRACT

The understanding of sour corrosion mechanisms is an important but still largely elusive target, especially as it pertains to the interaction between corrosion and corrosion product layer formation. The objective of this work was to investigate the effect of high temperature on the corrosion kinetics of carbon steel and the formation of corrosion product layers in sour environments. H_2S corrosion experiments were performed at 80°C, 120°C, 160°C, and 200°C with 4 d exposure. Linear polarization resistance was used to determine the corrosion rates. The corrosion products were identified by x-ray diffraction and examined by scanning electron microscopy together with energy dispersive spectroscopy. The results indicate that with the increase of temperature, the initial corrosion rates increased, then reached a steady state over time. Two distinct layers were found in the corrosion products. An inner iron oxide (postulated to be Fe_3O_4) layer was unexpectedly observed at every studied temperature, while the outer layer was identified as mackinawite, troilite, pyrrhotite, and pyrite at 80°C, 120°C, 160°C, and 200°C, respectively.

KEY WORDS: high-temperature corrosion, hydrogen sulfide, iron oxide, iron sulfide

INTRODUCTION

As the drilling and exploitation environments in oil and gas industry are becoming harsher and more aggressive, high-temperature hydrogen sulfide (H_2S) corrosion is more frequently encountered.[1-3] High temperatures and high pressures in association with H_2S corrosion may lead to many engineering challenges such as pipeline integrity, materials selection, and corrosion mitigation.

H_2S corrosion at low temperatures (<80°C) has been more widely studied,[4-6] and significant progress has been achieved to reveal the related general corrosion mechanisms. At elevated temperatures, however, H_2S corrosion has not been thoroughly studied and the understanding of the associated corrosion mechanisms is very limited. Overall, high temperature is fully expected to have a significant effect on the corrosion rate and formation/transformation of iron sulfide polymorphs.[7] Different corrosion product layers may also have different effects that lead to surface heterogeneity, the initiation of galvanic corrosion, and localized attack.

Therefore, in order to better understand, predict, and mitigate H_2S corrosion in oil and gas production at elevated temperatures, further experimental investigations are of great necessity. In this work, H_2S corrosion tests were conducted at 80°C, 120°C, 160°C, and 200°C to identify the effect of high temperature on the kinetics of corrosion and layer formation on mild steel in sour environments.

Submitted for publication: May 22, 2017. Revised and accepted: June 5, 2017. Preprint available online: June 5, 2017, http://dx.doi.org/10.5006/2523. Recipient of first place in the Marcel Pourbaix Corrosion Science category in the Student Poster Session at CORROSION 2017, March 2017, New Orleans, Louisiana.

‡ Corresponding author. E-mail: sg389813@ohio.edu.
* Institute for Corrosion and Multiphase Technology, Department of Chemical & Biomolecular Engineering, Ohio University, Athens, OH 45701.

ISSN 0010-9312 (print), 1938-159X (online)
17/000193/$5.00+$0.50/0

EXPERIMENTAL PROCEDURES

Experiments were performed in a 7 L Hastelloy[†] autoclave. A conventional three-electrode setup was used to conduct linear polarization resistance (LPR) measurements using a potentiostat. The working electrode was a cylindrical sample made from UNS K03014[(1)] (API 5L X65) carbon steel. A Pt-coated Nb counter electrode and a commercial Zr/ZrO_2 high-temperature, high-pressure pH probe were used. The pH probe reference also served as a reference electrode (exact potential still unknown) as long as its potential was stable at the desired test conditions.[8] Flat samples were also attached to a stabilized shaft using a polytetrafluoroethylene (PTFE)-coated Type 304 stainless steel (UNS S30400) wire. Before each experiment, the specimens were polished up to 600 grit sandpaper and rinsed with deionized water and isopropanol. A centrally located impeller with a rotation speed of 1,000 rpm was used to keep the solution fully mixed during each test.

The speciation at different temperatures was calculated according to an in-house water chemistry model,[9] as summarized in Table 1. The dissolved H_2S concentration $[H_2S]_{aq}$ was kept constant at 0.00385 mol/L, which corresponds to 0.10 bar H_2S at 80°C. After each test, the corroded samples were retrieved and characterized by x-ray diffraction (XRD), scanning electron microscopy/energy dispersive x-ray spectroscopy (SEM/EDS), and surface profilometry. Other experimental procedures and details can be found elsewhere.[9]

RESULTS AND DISCUSSION

Figure 1 shows the corrosion rates over time at 80°C, 120°C, 160°C, and 200°C as measured by LPR. It can be seen that the initial corrosion rates increased with increasing temperature, and then quickly decreased to stable corrosion rates of 4.1, 3.8, 1.8, and 2.5 mm/y, respectively, from lowest to highest temperature. Overall, the final steady-state corrosion rate decreased with temperature except at 200°C.

The corrosion products on the steel surface were characterized by XRD as shown in Figure 2. While mackinawite (FeS) was the main corrosion product detected at 80°C, troilite (FeS), pyrrhotite ($Fe_{1-x}S$, x = 0 to 0.17), and pyrrhotite/pyrite (FeS_2) became the dominant species as temperature was increased. With increasing temperature, the corrosion product became richer in sulfur; this is an indication of enhanced reaction kinetics for phase transformations.

The morphologies of the formed corrosion products were also characterized by SEM, as shown in Figure 3. The SEM for the 80°C specimen shows a mackinawite layer of 15-µm thickness. From the EDS line scan, the outer layer was identified to likely be an iron sulfide but an inner layer, which consisted mostly of iron and oxygen was assumed to be an iron oxide. At 120°C, the SEM shows troilite-like crystals on the surface and a much thicker layer (61 µm to 73 µm). At 160°C, pyrrhotite crystals were clearly observed on the

TABLE 1
Test Matrix

Parameter	Value			
Temperature (°C)	80	120	160	200
pH_2S (bar)	0.10	0.14	0.17	0.18
Initial pH	4.00			
$[H_2S]_{aq}$ (mol/L)	0.00385			
Duration (d)	4			

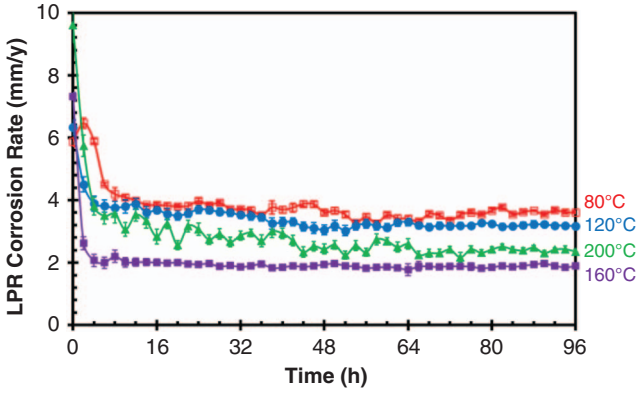

FIGURE 1. *Corrosion rate at different temperatures from LPR measurement, $[H_2S]_{aq}$ = 0.00385 mol/L, initial pH = 4.0, 4 d, B = 23 mV/decade.*

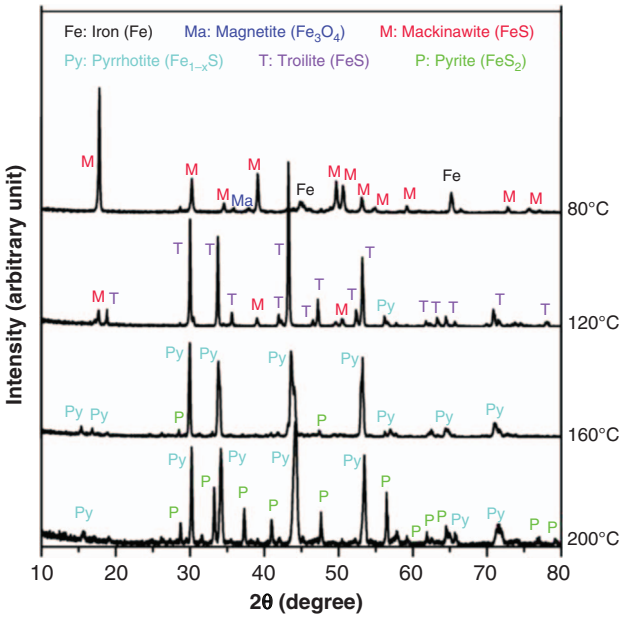

FIGURE 2. *XRD patterns of corrosion products on the steel surface at different temperatures, $[H_2S]_{aq}$ = 0.00385 mol/L, initial pH = 4.0, 4 d.*

[†] Trade name.
[(1)] UNS numbers are listed in *Metals and Alloys in the Unified Numbering System*, published by the Society of Automotive Engineers (SAE International) and cosponsored by ASTM International.

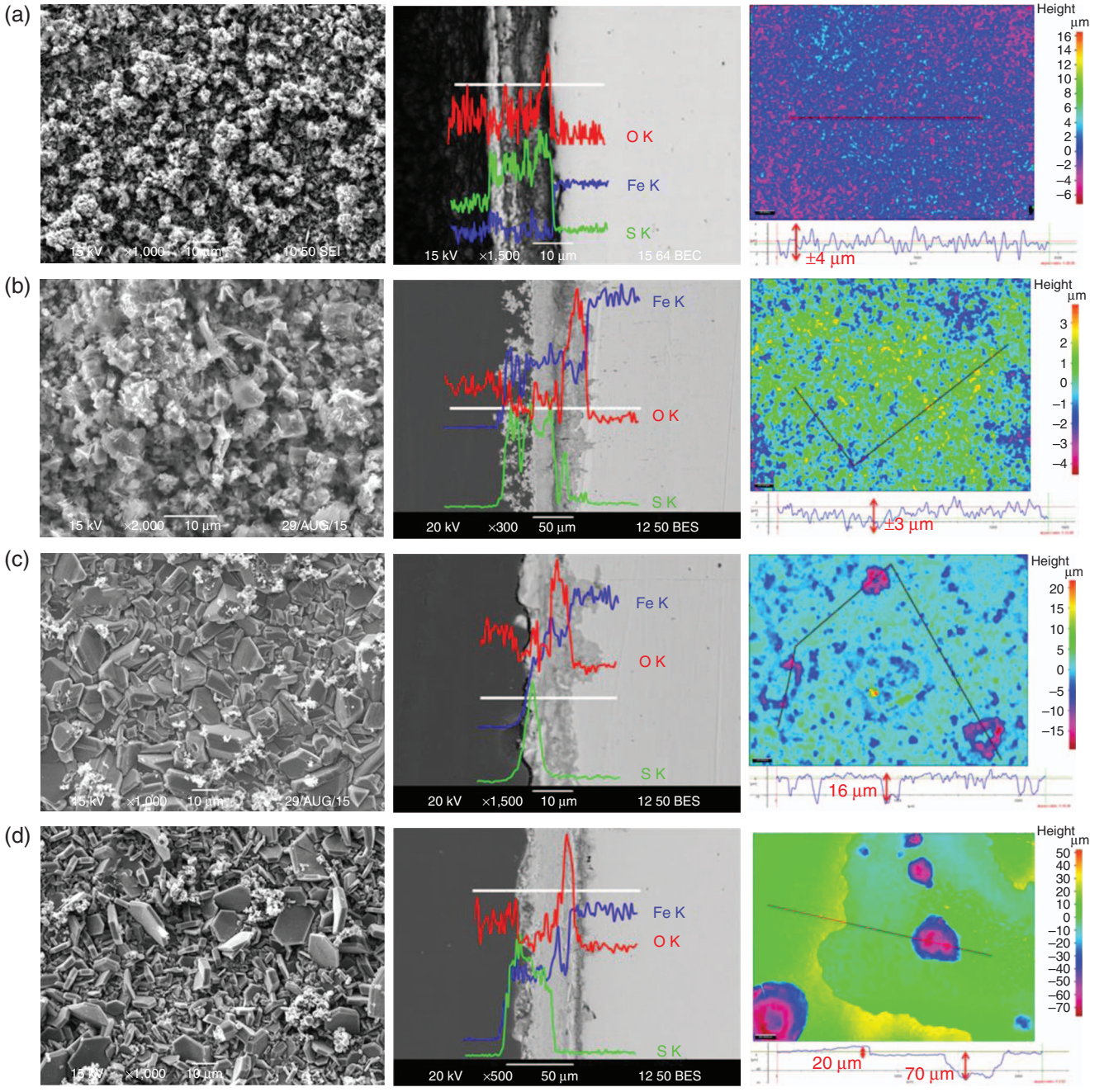

FIGURE 3. *SEM morphologies, cross sections, and surface profilometry at (a) 80°C, (b) 120°C, (c) 160°C, and (d) 200°C.*

surface. The corrosion products changed to planar flaky crystals at 200°C. All of the cross sections show a two-layer structure at every temperature tested: an inner layer comprising an iron oxide and an outer layer comprising an iron sulfide. However, the iron oxide was not detected by XRD as a result of the top layer being too thick and compact for XRD penetration.

Until now, iron oxide has not been given much attention as a corrosion product in H_2S corrosion environments. It is hypothesized that this iron oxide is magnetite (Fe_3O_4) because it was already identified at high temperatures in CO_2 environments.[10] The kinetics of Fe_3O_4 formation is very fast, making the scaling tendency (ST, the ratio of precipitation rate to corrosion rate) very high at high temperature. Fe_3O_4 can form on the metal surface according to the following reaction:

$$3Fe^{2+} + 4H_2O \Leftrightarrow Fe_3O_4 + 8H^+ + 2e^- \quad (1)$$

However, Fe_3O_4 is thermodynamically less stable than any of the iron sulfides. No Fe_3O_4 is thermodynamically expected in an Fe-H_2S-H_2O system.[9] Here, for an Fe-CO_2-H_2O system, from the Pourbaix diagram shown in Figure 4, it is seen that Fe_3O_4 is stable in a very

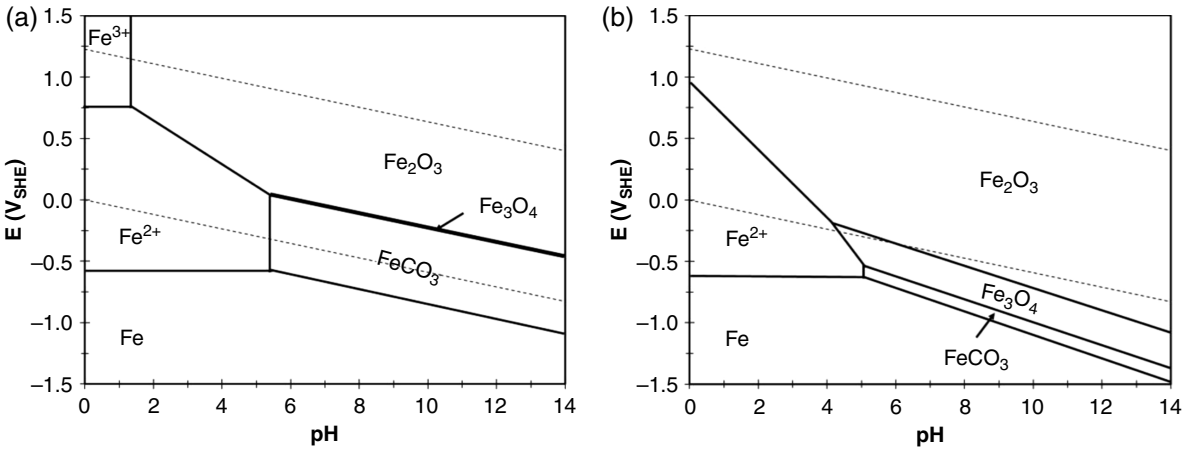

FIGURE 4. *Pourbaix diagram for Fe-CO_2-H_2O system at (a) 80°C and (b) 200°C, 1 bar CO_2 at 25°C.*

limited narrow area at potentials more positive than those for $FeCO_3$ at 80°C. When the temperature increases to 200°C, the stability region for Fe_3O_4 is greatly increased. New model for high-temperature corrosion of mild steel in aqueous H_2S environment at high temperature should also include Fe_3O_4 formation.

After removal of the corrosion products, the metal surface was characterized by profilometry, as shown in Figure 3. No obvious localized corrosion was observed at 80°C and 120°C. The surface was relatively smooth and the corrosion could be considered as uniform. However, at 160°C some small pits could be observed with approximately a 1.2 pitting ratio (ratio of maximum pit penetration rate to general corrosion rate) and 1.5 mm/y pit penetration rate. This does not constitute localized corrosion but may indicate initiation. At 200°C, many large pits appeared with a 3.2 pitting ratio and 8.2 mm/y pit penetration rate. The pitting ratio may not be a very accurate measure as pitting corrosion actually overwhelmed general corrosion. Because of severe localized corrosion at this temperature, the stable LPR corrosion rate appears to be a little higher than at 160°C (Figure 1). These results fit with Ning, et al.'s previous work[11] where it was found that pyrite formation triggers the occurrence of localized attack.

SUMMARY

❖ Sour corrosion experiments were conducted successfully at 80°C, 120°C, 160°C, and 200°C. Initial corrosion rates increased with increasing temperature. Final corrosion rates, after 4 d of exposure, remained high at between 2 mm/y and 4 mm/y. The corrosion product comprised two distinct layers: an inner layer, close to the steel substrate, and an outer layer, on the solution's side. The inner layer was identified as an iron oxide (postulated to be Fe_3O_4) even though it is not thermodynamically stable in the conditions tested. The outer layer was mainly composed of iron sulfide: mackinawite, troilite, pyrrhotite, and pyrite at 80°C, 120°C, 160°C, and 200°C, respectively.

ACKNOWLEDGMENTS

The authors would like to express sincere appreciation to the following industrial sponsors for their financial support and direction: Anadarko, Baker Hughes, BP, Chevron, China National Offshore Oil Corporation, ConocoPhillips, DNV GL, ExxonMobil, M-I SWACO, Occidental Oil Company, Petroleum Institute, PTT, Saudi Aramco, Shell Global Solutions, SINOPEC, TOTAL, TransCanada, and WGK.

REFERENCES

1. G. DeBruijin, *Oilfield Rev.* 20 (2008): p. 46.
2. H.J. Chen, "High Temperature Corrosion Inhibition Performance of Imidazoline and Amide," CORROSION 2010, paper no. 0035 (Houston, TX: NACE International, 2010).
3. S.S. Prabha, *Eur. Chem. Bull.* 3 (2014): p. 300.
4. H. Ma, X. Cheng, G. Li, S. Chen, Z. Quan, S. Zhao, L. Niu, *Corros. Sci.* 42 (2000): p. 1669.
5. W. Sun, S. Nešić, S. Papavinasam, "Kinetics of Iron Sulfide and Mixed Iron Sulfide/Carbonate Scale Precipitation in CO_2/H_2S Corrosion," CORROSION 2006, paper no. 644 (Houston, TX: NACE, 2006).
6. J. Tang, Y. Shao, J. Guo, T. Zhang, G. Meng, F. Wang, *Corros. Sci.* 52 (2010): p. 2050.
7. Y. Qi, H. Luo, S. Zheng, C. Chen, Z. Lv, M. Xiong, *Int. J. Electrochem. Sci.* 9 (2014): p. 2101.
8. R. Thodla, F. Gui, K. Evans, C. Joia, I.P. Baptista, "Corrosion Fatigue Performance of Super 13 CR, Duplex 2205 and 2507 for Riser Applications," CORROSION 2010, paper no. 312 (Houston, TX: NACE, 2010).
9. S. Gao, P. Jin, B. Brown, D. Young, S. Nešić, M. Singer, *Corrosion* 73 (2017): p. 915.
10. T. Tanupabrungsun, D. Young, B. Brown, S. Nešić, "Construction and Verification of Pourbaix Diagrams for CO_2 Corrosion of Mild Steel Valid up to 250°C," CORROSION 2012, paper no. 1418 (Houston, TX: NACE, 2012).
11. J. Ning, Y. Zheng, B. Brown, D. Young, S. Nešić, *Corrosion* 73 (2017): p. 155.